

Determination of mercury(II) by surface-enhanced Raman scattering spectroscopy based on thiol-functionalized silver nanoparticles

Yang Chen · Lihang Wu · Yanhua Chen · Ning Bi ·
Xia Zheng · Haibo Qi · Meihong Qin · Xue Liao ·
Hanqi Zhang · Yuan Tian

Received: 27 October 2011 / Accepted: 3 February 2012 / Published online: 28 February 2012
© Springer-Verlag 2012

Abstract Silver nanoparticles (Ag NPs) modified with sodium 2-mercaptoethanesulfonate (mesna) exhibit strong surface-enhanced Raman scattering (SERS). Their specific and strong interaction with heavy metal ions led to a label-free assay for Hg(II). The covalent bond formed between mercury and sulfur is stronger than the one between silver and sulfur and thus prevents the adsorption of mesna on the surface of Ag NPs. This results in a decrease of the intensity of SERS in the presence of Hg(II) ions. The Raman peak at 795 cm^{-1} can be used for quantification. The effect of the concentration of mesna, the concentration of sodium chloride, incubation time and pH value on SERS were optimized. Under the optimal conditions, the intensity of SERS decreases with increasing concentration of Hg(II). The decrease is linear in the 0.01 and $2\text{ }\mu\text{mol L}^{-1}$ concentration range, with a correlation coefficient (R^2) of 0.996 and detection limit ($S/N=3$) is $0.0024\text{ }\mu\text{mol L}^{-1}$. The method was successfully applied to the determination of the Hg(II) in spiked water samples.

Keywords Surface-enhanced Raman scattering · Hg^{2+} · Mesna · Ag NPs

Introduction

Mercury is one of the most toxic elements and highly toxic because it has serious medical effects on human beings and ecological safety, such as brain damage, kidney failure, and various cognitive and motion disorders [1, 2]. Thus, a rapid and efficient method for determination of Hg^{2+} is important. In general, absorption spectrometry is one of the most popular methods to detect heavy metals. The absorption efficiency, selectivity, equilibrium time, regeneration, and stability usually depend on the material characteristics of the absorbents [3, 4]. Inductively coupled plasma mass spectrometry (ICPMS) is a powerful technique for the determination of heavy metal ions. However, ICPMS is rather expensive, complex, and not suitable for on-site analysis [5]. Several sensors have been applied for determination of mercury in environmental samples. Because the absorptivity of Au NPs in visible-region are often higher than those of organic dyes [6, 7], Au NPs-based methods for visual or colorimetric sensing of Hg^{2+} have become of great interest. For example, Chansuvarn [8] used gold nanoparticles stabilized with a dithia-diaza ligand for detection of mercury(II) ion and Tian group [9] used chemodosimeter-functionalized Au NPs for detection of Hg^{2+} . The colorimetric methods are simple. The complex and expensive instruments are not required. But most of these methods involve a color change, which results in the decrease of the sensitivity due to the interference from background colors [10]. The preparation of these colorimetric sensors involves several steps, which is complex and relatively expensive. Fluorescence spectrophotometry can be applied for the determination of the analytes at low concentration. Some new methods based on fluorescence-based probes and sensors for determination of

Electronic supplementary material The online version of this article (doi:10.1007/s00604-012-0777-6) contains supplementary material, which is available to authorized users.

Y. Chen · L. Wu · Y. Chen · N. Bi · X. Zheng · H. Qi · M. Qin ·
X. Liao · H. Zhang · Y. Tian (✉)
College of Chemistry, Jilin University,
Changchun 130012, Peoples Republic of China
e-mail: tianyuan@jlu.edu.cn

Hg²⁺ have been reported, such as DNAzymes [11], oligonucleotide platforms [12], CdTe quantum dots [13]. However, nucleic acid or enzyme sensors are rather costly. Most of the quantum dots tend to have narrow excitation spectra and often exhibit broad emission band with red tailing. Thus, it is necessary to develop a new method to meet the requirement for the determination of Hg²⁺ from wastewater.

It is well known that Raman spectroscopy emerged as fast and non-invasive determination of adulterants in many fields [14–17]. Signals in conventional Raman spectroscopy are very weak and great progress has been made in the development of surface-enhanced Raman scattering (SERS) spectroscopy. SERS is an exceptionally analytical technique for its high sensitivity, fluorescence-quenching property and fingerprint information about the chemical structures. Recently, SERS spectrometry has been developed as a potential trace method and is widely applied for detecting single molecule in chemistry, biology and medicine. When Raman scattering takes place on molecules at the surface or in the close vicinity of noble metal surfaces, such as gold and silver, a very high enhancement (up to 10¹⁴–10¹⁵) is required [18–22]. Theoretically, the huge local electromagnetic field is attributed to the so-called hot spots, which may be junctions between nanostructures. SERS substrates consist of various metallic nanostructures, including roughened gold and silver electrodes, evaporated thin films, Au or Ag nanoparticles and Au/Ag core-shell nanostructures [23]. The noble-metal SERS substrate not only provides enhanced Raman signals but also quenches the fluorescence generated by many organic colorants. The Ag NPs as SERS-active sites have been used due to the unique electronic, optical, and chemical properties. Ag NPs are simple to prepare, with good control of size and shape and widely used in electronics [24], sensing [25], biology [26] and SERS [27, 28].

In this work, a method for determination of Hg²⁺ with mesna modified Ag NPs was described. When mesna molecules are adsorbed on Ag NPs by Ag-S covalent bond, the SERS signals increased significantly due to electromagnetic and chemical enhancement factors [29, 30]. However, after the addition of Hg²⁺, the mesna was released from the surface of Ag NPs, which caused the decrease of SERS intensity. Hg²⁺ can be directly determined by monitoring the shift of SERS intensity.

Materials and methods

Reagents and instruments

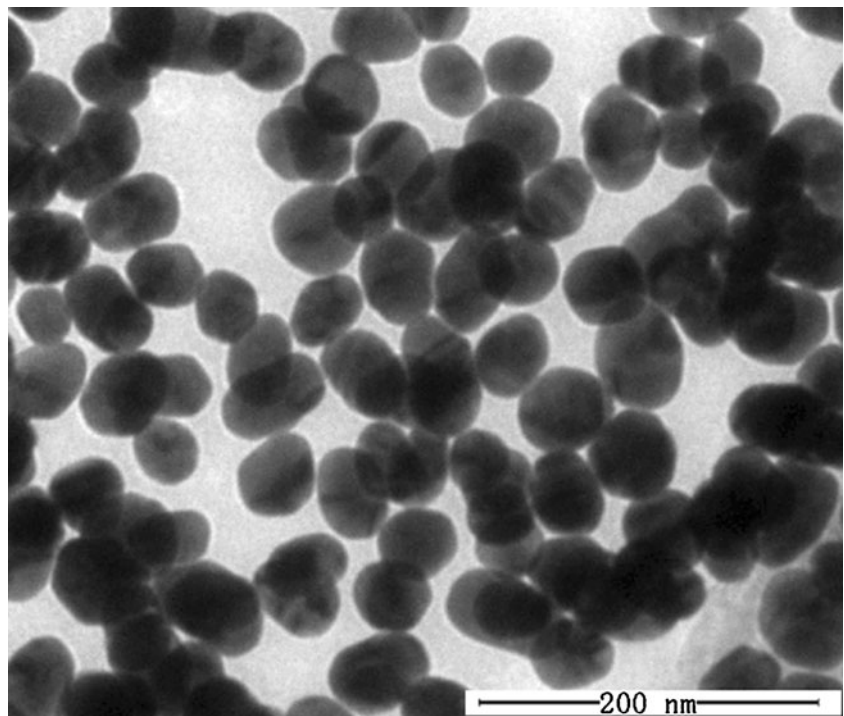
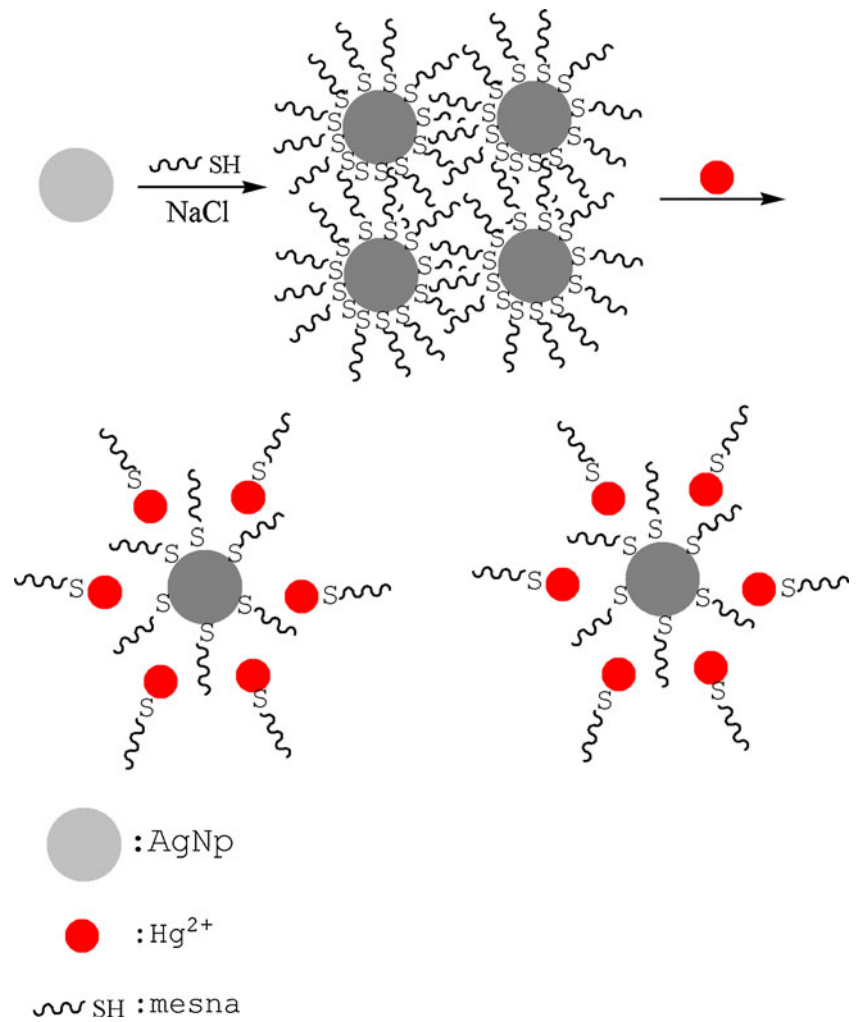
Sodium 2-mercaptoethanesulfonate (mesna), silver nitrate (AgNO₃, 99%) and mercury(II) chloride were purchased from Beijing Ding Guo Biotech. Co. Ltd., China ([http://](http://www.dingguo.com)

www.dingguo.com). The stock solution of Hg(II) was prepared by dissolving HgCl₂ in ultrapure water containing several drops of HCl. The working solution of Hg²⁺ was prepared by diluting the stock solution with ultrapure water. The metal salts KCl, NaBr, BaCl₂·2H₂O, NiCl₂·6H₂O, Na₂HPO₄·12H₂O, MgCl₂·6H₂O, CaCl₂·2H₂O, Na₂SO₄, Na₂CO₃, Al₂(SO₄)₃·18H₂O, FeCl₂·4H₂O, CuCl₂·2H₂O, Pb(CH₃COO)₂·3H₂O, MnSO₄·H₂O, COCl₂·6H₂O, FeCl₃·6H₂O, CdSO₄·8/3H₂O, CrK(SO₄)₂·12H₂O, AgNO₃, and SnCl₂·2H₂O were purchased from Beijing Chemical Reagent Company (<http://www.18show.cn/zt340222/Intro.html>). Britton–Robinson buffer containing 0.04 mol L⁻¹ H₃BO₃, 0.04 mol L⁻¹ H₃PO₄ and 0.04 mol L⁻¹ CH₃COOH was adjusted to the desired pH with 0.2 mol L⁻¹ NaOH. The buffer was used to control the acidity of the sample solution. All glassware was cleaned with freshly prepared aqua regia (HCl/HNO₃, 3/1, v/v) and rinsed thoroughly with ultrapure water prior to use. Other reagents used here were of analytical reagent grade and used without further purification or treatment.

The transmission electron microscope (TEM) image was obtained with a Hitachi H 800 transmission electron microscope (<http://www.labbase.net/>) operated at an accelerating voltage of 200 kV. The samples for TEM images were prepared by dropping the solutions containing Ag NPs on the carbon-coated copper grid and drying at room temperature. Absorption spectra were recorded on an Astralian GBC Cintra 10e UV–vis–NIR spectrometer within the wavelength range from 300 to 800 nm. Raman spectra were obtained using a BTR 111 Mini-Ram B&W Tek, Inc. (<http://www.shtqsw.com>) with a 1 cm quartz cell and the wavelength of the emission line for the laser is 785 nm. The laser power was chosen as 70 mW. Exposure time used for data collection was typically 10 s. The datum processing was operated by using Origin 6.0 software.

Preparation of Ag NPs

The Ag NPs were prepared according to reported method [31]. First, 90 mg of AgNO₃ was dissolved in 500 mL of ultrapure water and heated to boiling. Then 10 mL of 1% sodium citrate solution was added into the boiling AgNO₃ solution with vigorous stirring. The mixed solution was kept at boiling for 1 h. The green-gray Ag NPs were obtained and the average diameter of the Ag NPs is about 50 nm. The transmission electron microscopy (TEM) image of the Ag NPs is shown in Fig. 1. The resulting colloid was yellowish gray with an absorption maximum at 420 nm and pH of 7.8. Finally, the Ag NPs solution was allowed to cool down to room temperature for further experiments.

Fig. 1 TEM image of Ag NPs**Fig. 2** Schematic illustration of the determination process

Determination of Hg^{2+}

2 mL of sample solution, 50 μL of $6.4 \times 10^{-5} \text{ mol L}^{-1}$ mesna solution and 800 μL of Ag NPs solution were added into the 5 mL colorimetric tube. Then, 35 μL of 2 mol L^{-1} NaCl solution and 115 μL of BR buffer solution were added into the mixed solution. The resulting solution was kept at room temperature for 6 min. A quantitative analysis was performed based on the measured peak area at 795 cm^{-1} in SERS spectrum. The SERS intensity was expressed in the peak area. All the experiments were performed in triplicate.

Results and discussions

Mechanistic basis for the system

Figure 2 shows the schematic illustration for determining mercury. Mesna molecules can adsorb on the surface of Ag NPs by $-\text{SH}$ group, which can result in the enhancement of SERS signals. The mesna molecules are released from the surface of Ag NPs in the presence of mercury(II), which caused a decrease in the observed SERS signal. The experimental results indicated that SERS signal decreased with the increase of Hg^{2+} concentration. Thus, a quantitative determination for Hg^{2+} was developed.

SERS spectra of mesna modified Ag NPs

A typical SERS spectrum of mesna modified Ag NPs is shown in Fig. 3. The band in SERS spectrum located at 795 cm^{-1} is attributed to the C-S stretching vibration and sulfur is from the sulfonic group. The other major bands in the SERS spectrum are located at 540, 591, 704, 1,058 and $1,295 \text{ cm}^{-1}$. All of the bands are characteristic for

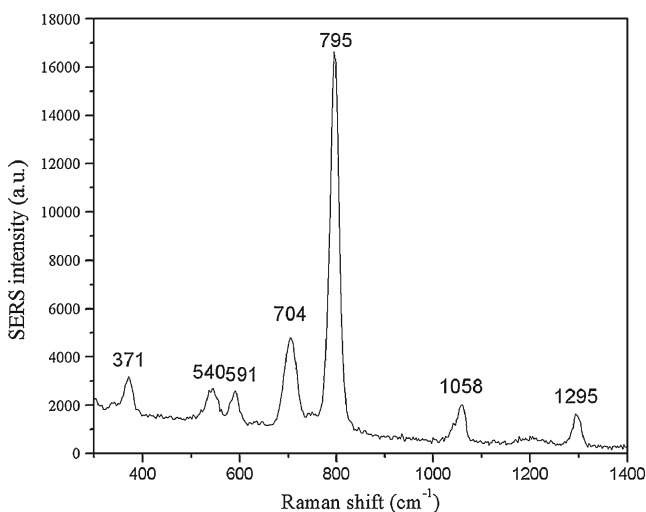


Fig. 3 SERS spectrum of mesna-Ag NPs system

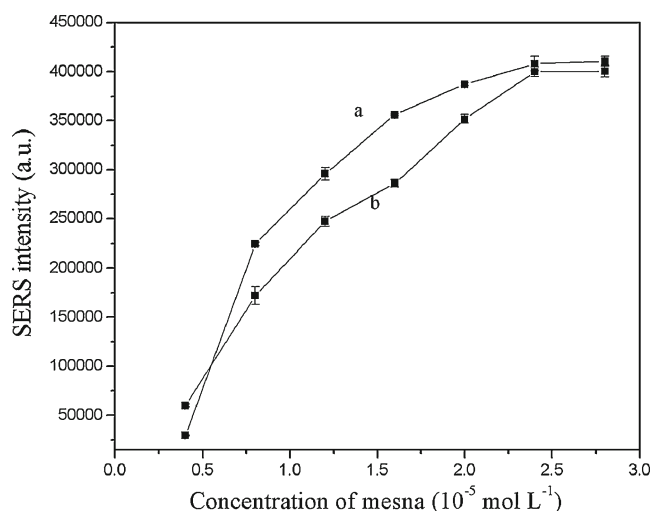


Fig. 4 Effect of mesna concentration on the SERS intensity of mesna-Ag NPs system in the absence (a) and presence (b) of Hg^{2+} . Concentration of NaCl, 0.035 mol L^{-1} . Concentration of Hg^{2+} , $0.8 \mu\text{mol L}^{-1}$. pH, 7

chemisorbed mesna molecules. The bands at 540 and 591 cm^{-1} are attributed to the C-C stretching vibrations. The band at 540 cm^{-1} is characteristic of the gauche (G) conformer of the Ag-S-C-C chain, whereas the band at 591 cm^{-1} is typical of the trans (T) conformer. The band at 704 cm^{-1} is also due to the C-S stretching vibration but sulfur is from the thiol group. The 704 cm^{-1} band is characteristic of chemisorbed mesna molecules having a trans conformation of the Ag-S-C-C and the bands at $1,058$ and $1,295 \text{ cm}^{-1}$ are due to the symmetric and anti symmetric (SO_3^{2-}) stretch, respectively [32–35].

There is not any observable S-H stretching vibration band in the range of $2,500\text{--}2,600 \text{ cm}^{-1}$. It suggests that the S-H

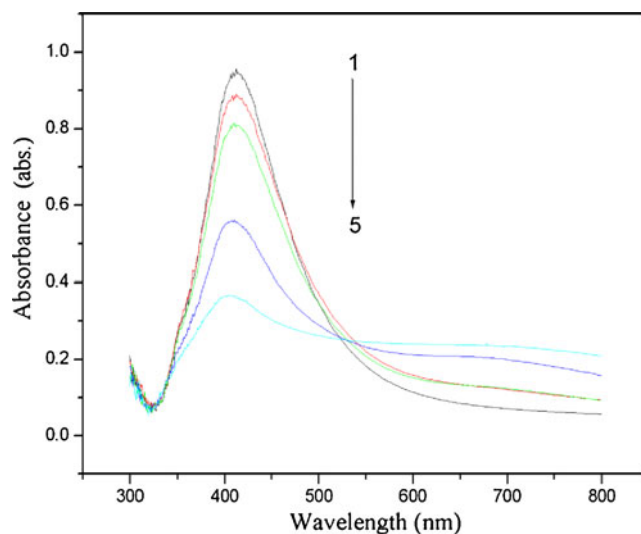


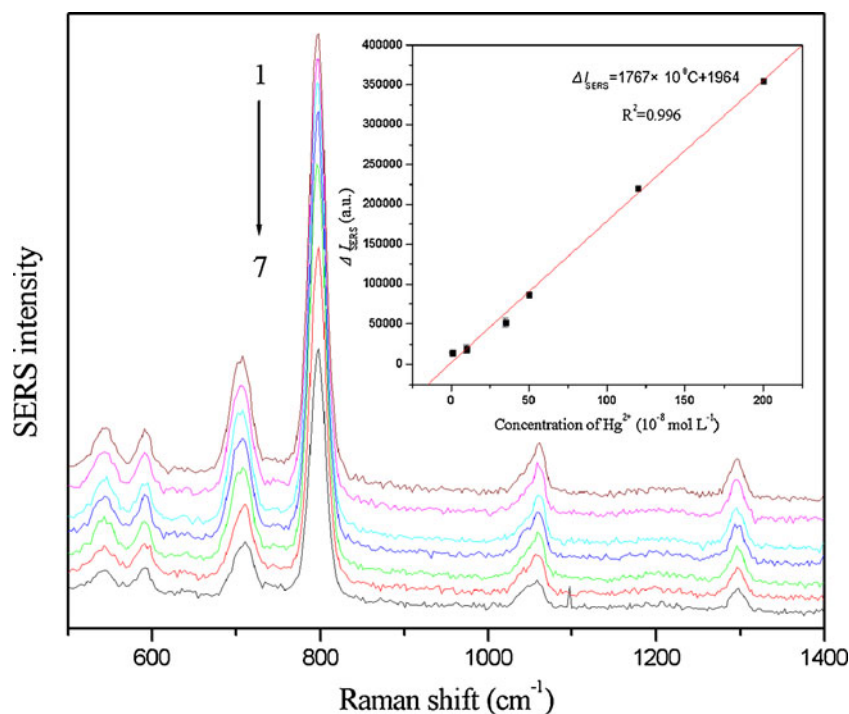
Fig. 5 Absorption spectra of the Ag NPs in the presence of different concentrations of NaCl. Concentrations of NaCl: (1) 0.0, (2) 0.014, (3) 0.027, (4) 0.036, (5) 0.042 mol L^{-1}

Table 1 Influence of potentially interfering ions

Potentially interfering ions	Concentration ($\times 10^{-7}$ mol L $^{-1}$)	Relative error (%)
K $^{+}$, Cl $^{-}$	800.0	+8.1
Na $^{+}$, Br $^{-}$	800.0	-11.7
Pb $^{2+}$, CH $_3$ COO $^{-}$	800.0	-3.8
Mn $^{2+}$, SO $_4^{2-}$	800.0	-1.9
Co $^{2+}$, Cl $^{-}$	800.0	3.7
Fe $^{3+}$, Cl $^{-}$	800.0	-7.5
Cd $^{2+}$, SO $_4^{2-}$	800.0	+1.0
Na $^{+}$, HPO $_4^{2-}$	400.0	+1.3
Mg $^{2+}$, Cl $^{-}$	400.0	+2.1
Ca $^{2+}$, Cl $^{-}$	400.0	+3.8
Na $^{+}$, SO $_4^{2-}$	400.0	-0.8
Na $^{+}$, CO $_3^{2-}$	400.0	+5.9
Al $^{3+}$, SO $_4^{2-}$	400.0	+1.5
Fe $^{2+}$, Cl $^{-}$	400.0	+9.4
Cr $^{3+}$, SO $_4^{2-}$	80.0	-13.1
Ag $^{+}$, NO $_3^{-}$	8.0	-3.2
Sn $^{2+}$, Cl $^{-}$	8.0	+9.4
Ba $^{2+}$, Cl $^{-}$	4.0	-4.2
Ni $^{+}$, Cl $^{-}$	4.0	+1.3
Cu $^{2+}$, Cl $^{-}$	4.0	-3.4

bond is cleaved and adsorbed onto the surface of Ag NPs. In some complexes the Ag-S vibration was reported at a frequency as high as 363 cm $^{-1}$ [36]. So, in the present study the 371 cm $^{-1}$ band may be assigned to the Ag-S stretching mode.

Fig. 6 SERS spectra of mesna-Ag NPs system in the presence of Hg $^{2+}$. Inset shows the relationship between ΔI_{SERS} and the concentration of Hg $^{2+}$. Concentrations of Hg $^{2+}$: (1) 0.1×10^{-7} , (2) 1×10^{-7} , (3) 3.5×10^{-7} , (4) 5×10^{-7} , (5) 12×10^{-7} , (6) 20×10^{-7} mol L $^{-1}$. Concentration of mesna, 1.6×10^{-5} mol L $^{-1}$. Concentration of NaCl, 0.035 mol L $^{-1}$. pH, 7



The optimization of experimental conditions

Effect of mesna concentration

The effect of mesna concentration on the SERS intensity was investigated and is shown in Fig. 4. When the concentrations of the mesna vary from 0.4×10^{-5} to 2.4×10^{-5} mol L $^{-1}$, the SERS intensities increase with the increase of the concentrations of mesna and change insignificantly until 2.8×10^{-5} mol L $^{-1}$. The shift of SERS intensity is expressed as $\Delta I_{\text{SERS}} = I_{\text{SERS}}^0 - I_{\text{SERS}}$. Here I_{SERS}^0 and I_{SERS} are the SERS intensities of the system in the absence and presence of Hg $^{2+}$, respectively. The ΔI_{SERS} intensity reaches the maximum when the concentration of mesna is 1.6×10^{-5} mol L $^{-1}$. Therefore, the 1.6×10^{-5} mol L $^{-1}$ mesna was selected for subsequent work.

Effect of pH value

The effect of pH on the SERS intensity was investigated in the pH value range from 4 to 10. As shown in Fig. S1 (Electronic Supplementary Materials, ESM) the ΔI_{SERS} values in the presence and the absence of Hg $^{2+}$ change slightly with the change of pH value. So pH value 7 was selected for the determination of Hg $^{2+}$.

Effect of incubation time

The influence of incubation time of mesna modified Ag NPs was also investigated. As shown in Fig. S2 (ESM), the

Table 2 Comparison of previously reported method with the present method for the detection of Hg²⁺

Method	Reagent	LOD ($\mu\text{mol L}^{-1}$)	Linear range ($\mu\text{mol L}^{-1}$)	References
SERS	Mesna modified Ag NPs	2.4×10^{-3}	0.01–2	This work
Colorimetric	Gold nanoparticles stabilized with a dithia-diaza ligand	35×10^{-3}	0–9	[8]
Spectrophotometry	C[6]/SiO ₂ /CdTe nanoparticles	1.55×10^{-3}	$2\text{--}14 \times 10^{-3}$	[13]
SERS	Trimercaptotriazine-modified gold nanoparticles	–	0.2–2	[39]
SPR	Mercury-specific oligonucleotide (MSO)	5×10^{-3}	$5\text{--}375 \times 10^{-3}$	[40]
LSPR scattering	Hg ²⁺ -DNA complex	1.0×10^{-3}	$0.4\text{--}6.0 \times 10^{-1}$	[41]
Electrochemical	Oligonucleotide	0.1	0.1–2	[42]
CVAAS	Cyanex 923 as a sorbent	0.997×10^{-6}	$0.00997\text{--}0.997 \times 10^{-2}$	[43]
FRET	CdTe QDs and butyl-rhodamine B	20.3×10^{-3}	0.0625–2.5	[44]
HEMT	Thioglycolic acid functionalized Au-gated AlGaIn/GaN	1.5×10^{-2}	0.015–0.04	[45]
Fluorescence quenching	Bi-color CdTe quantum dots multilayer films	4.5×10^{-3}	0.01–1.0	[46]

LSPR localized surface plasmon resonance; CVAAS cold vapor atomic absorption spectrometry; FRET fluorescence resonance energy transfer; HEMT high electron mobility transistor

reaction between mesna modified Ag NPs and Hg²⁺ occurs rapidly at room temperature. The ΔI_{SERS} values in the presence and the absence of Hg²⁺ change slightly within 9 min. The incubation time of 6 min was selected to achieve stability SERS signal in the experiment.

Effect of sodium chloride concentration

The concentration of sodium chloride plays an important role in the experiment. Fig. S3 (ESM) shows the dependence of chemical enhancement on the sodium chloride concentration. The SERS peak at 795 cm^{-1} was chosen. It can be seen from Fig. S3 that the SERS intensity increases with the increase of NaCl concentration and reaches a maximum at 0.035 mol L^{-1} . When the concentration of NaCl is higher than 0.035 mol L^{-1} , the SERS intensity decreases slightly. It is well known that NaCl is used as an aggregating agent for Ag NPs in the enhancement process, and the concentration of NaCl can influence the aggregation degree of Ag NPs.

It is generally agreed that two fundamentally different mechanisms dominated in the SERS phenomenon, one is electromagnetic (EM) enhancement and the other one is the resonance-like charge-transfer (CT) enhancement. The salts can improve electromagnetic enhancement caused by particle aggregation, anion-induced adsorption/reorientation of

analyte and an charge transfer contribution. First, the aggregated particle widens the plasmon band so that a wide range of excitation laser wavelength can be used for electromagnetic enhancement. Aggregation processes can produce junctions between particles, and these junctions act as electromagnetic hot spots. The analyte can easily adsorb onto those hot spots during the aggregation processes. Thus, the analyte has to be present during the particle aggregation process so that the analyte molecules have a higher chance of adsorbing on those hot spots [18]. Second, Cl⁻ is chemisorbed onto the colloidal surface owing to their high affinity for silver and can change the surface morphology of the SERS-active substrate [37]. These latter are active sites for the formation of molecule/metal complexes by charge-transfer effect that leads to an increase in the interaction between mesna and the Ag NPs [38].

In order to understand the effect of NaCl, the absorption spectra of Ag NPs were measured in the absence and presence of NaCl. The absorption spectra can provide the aggregation degree of Ag NPs. As shown in Fig. 5, with the increase of NaCl concentration, the intensity of the surface plasmon absorption band decreases and the absorption peaks of Ag NPs are broadened. The surface plasmon band is close to the laser excitation wavelength of 785 nm, which can increase the electromagnetic enhancement effect.

Table 3 Analytical results for the three real samples

Samples	Added ($\mu\text{mol L}^{-1}$)	Found ($\mu\text{mol L}^{-1}$)	Recovery ($n=3$, %)	RSD ($n=3$, %)
South Lake	0.2	0.20	100.0	0.3
	1.2	1.06	88.3	1.5
Groundwater	0.2	0.23	115.0	0.5
	1.2	0.95	79.2	1.6
Jingyue Lake	0.2	0.16	80.0	2.3
	1.2	0.86	71.6	1.1

Selectivity of the sensing system

To investigate the selectivity of the present method, several metal ions were tested under the same experimental conditions when the concentration of Hg^{2+} was $4 \times 10^{-7} \text{ mol L}^{-1}$. The experimental results are listed in Table 1. Most of the metal ions at high concentrations have a little influence on the SERS intensity of the system. Mesna modified Ag NPs exhibit high selectivity for the determination of Hg^{2+} in the presence of a variety of competitive ions. The affinity between Hg^{2+} and -S is stronger than those between other ions and -S. Hg^{2+} ions are expected to bind with mesna modified Ag NPs through cooperative metal–ligand interaction to form a stable complex. It is can be concluded that mesna modified Ag NPs can be used to selectively determine Hg^{2+} in practical samples.

Determination of Hg^{2+}

Under the optimal conditions, different concentrations of Hg^{2+} were determined. Figure 6 shows the representative SERS spectra of mesna and Ag NPs system in the presence of Hg^{2+} . It is can be seen from Fig. 6 that the intensity of SERS decreases with the increase of Hg^{2+} concentration. The intensity of the Raman peak at 795 cm^{-1} was used for the quantification. Inset shows the SERS responses in the presence of Hg^{2+} at different concentrations. ΔI_{SERS} is directly proportional to the concentration of Hg^{2+} in the range of $1\text{--}200 \times 10^{-8} \text{ mol L}^{-1}$ with a correlation coefficient (R^2) of 0.996. The regression equation is $\Delta I_{\text{SERS}} = 1,767 \times 10^8 C + 1,964$ (C : mol L^{-1}). The detection limit, which corresponds to signal-to-noise ratio 3, is $0.0024 \mu\text{mol L}^{-1}$. For comparison, the experimental results for the determination of Hg^{2+} obtained by some other methods are listed in Table 2. Compared with other methods when this method is applied the operation is simpler and the selectivity is superior.

Analysis of environmental water samples

The application of the present method was evaluated for determination of Hg^{2+} in three water samples. Accuracy of this method was evaluated by determining the recoveries of Hg^{2+} in the water samples. Three water samples were collected from South Lake, Groundwater and Jinyue Lake in Changchun respectively. The samples were spiked with Hg^{2+} at two concentration levels, filtered through a $0.22 \mu\text{m}$ membrane and then analyzed by SERS spectroscopy. The results are summarized in Table 3. It is can be seen from Table 3 that the recoveries of Hg^{2+} at two concentration levels are between 71% and 115%, the RSDs are between 0.3% and 2.3%. The results reveal that the present method can be applied to the analysis of real water samples.

Conclusion

The mesna-modified Ag NPs can be used as probe to determine mercury ions. This method will have several advantages: a) it can be 2–3 orders of magnitude more sensitive than the usual colorimetric method; b) it exhibits excellent selectivity; c) it takes only 6 min to determine mercury in aqueous solution; d) only a low-cost and portable device is needed. This method is simple and convenient. Therefore, this method might provide a potential tool for the sensitive determination of Hg^{2+} in biological and environmental samples.

References

- Vupputuri S, Longnecker MP, Daniels JL, Guo X, Sandler DP (2005) A blood mercury level and blood pressure among US women: results from the National Health and Nutrition Examination Survey 1999–2000. *Environ Res* 97:195–200
- Virtanen JK, Rissanen TH, Voutilainen S, Tuomainen TP (2007) Mercury as a risk factor for cardiovascular diseases. *J Nutr Biochem* 18:75–85
- Yang H, Xu R, Xue X, Li F, Li G (2008) Hybrid surfactant-templated mesoporous silica formed in ethanol and its application for heavy metal removal. *J Hazard Mater* 152:690–698
- Wu ShJ, Li FT, Wu YN, Xu R, Li GT (2010) Preparation of novel poly(vinyl alcohol)/ SiO_2 composite nanofiber membranes with mesostructure and their application for removal of Cu^{2+} from waste water. *Chem Commun* 46:1694–1696
- Li YF, Chen ChY, Li B, Sun J, Wang JX, Gao YX, Zhao YL, Chai ZhF (2006) Elimination efficiency of different reagents for the memory effect of mercury using ICP-MS. *J Anal At Spectrom* 21:94–96
- Moores A, Goettmann F (2006) The plasmon band in noble metal nanoparticles: an introduction to theory and applications. *New J Chem* 30:1121–1132
- Kim YJ, Johnson RC, Hupp JT (2001) Gold nanoparticle-based sensing of “spectroscopically silent” heavy metal ions. *Nano Lett* 1:165–167
- Chansuvarn W, Imyim A (2011) Visual and colorimetric detection of mercury(II) ion using gold nanoparticles stabilized with a dithiadiazia ligand. *Microchim Acta*. doi:10.1007/s00604-011-0691-3
- Leng B, Zou L, Jiang JB, Tian H (2009) Colorimetric detection of mercuric ion (Hg^{2+}) in aqueous media using chemodosimeter-functionalized gold nanoparticles. *Sens A actuators B* 140:162–169
- Wang YL, Li D, Ren W, Liu ZJ, Dong ShJ, Wang EK (2008) Ultrasensitive colorimetric detection of protein by aptamer–Au nanoparticles conjugates based on a dot-blot assay. *Chem Commun* 2520–2522
- Thomas JM, Ting R, Perrin DM (2004) High affinity DNA zyme-based ligands for transition metal cations—a prototype sensor for Hg^{2+} . *Org Biomol Chem* 2:307–312
- Ono A, Togashi H (2004) Highly selective oligonucleotide-based sensor for mercury(II) in aqueous solutions. *Angew Chem Int Ed* 43:4300–4302
- Li T, Zhou YY, Sun JY, Tang DB, Guo SX, Ding XP (2011) Ultrasensitive detection of mercury(II) ion using CdTe quantum dots in sol-gel-derived silica spheres coated with calix[6]arene as fluorescent probes. *Microchim Acta* 175:113–119

14. Weng YM, Weng RH, Tzeng CY, Chen WL (2003) Structural analysis of triacylglycerols and edible oils by near-infrared Fourier transform Raman spectroscopy. *Appl Spectrosc* 57:413–418
15. Muik B, Lendl B, Diaz AM, Ayora-Cañada MJ (2003) Direct reagent-free determination of free fatty acid content in olive oil and olives by Fourier transform Raman spectrometry. *Anal Chim Acta* 487:211–220
16. Ellis DI, Broadhurst D, Clarke SJ, Goodacre R (2005) Rapid identification of closely related muscle foods by vibrational spectroscopy and machine learning. *Analyst* 130:1648–1654
17. Mulvihill M, Tao A, Benjauthrit K, Arnold J, Yang PD (2008) Surface-enhanced Raman spectroscopy for trace arsenic detection in contaminated water. *Angew Chem Int Ed* 47:6456–6460
18. Jana BNR, Pal T (2007) Anisotropic metal nanoparticles for use as surface-enhanced Raman substrates. *Adv Mater* 19:1761–1765
19. Le Ru EC, Etchegoin PG, Meyer M (2006) Enhancement factor distribution around a single surface-enhanced Raman scattering hot spot and its relation to single molecule detection. *J Chem Phys* 125:204701–204713
20. Camden JP, Dieringer JA, Wang YM, Masiello DJ, Marks LD, Schatz GC, Van Duyne RP (2008) Probing the structure of single-molecule surface-enhanced Raman scattering hot spots. *J Am Chem Soc* 130:12616–12617
21. Lee SJ, Morrill AR, Moskovits M (2006) Hot spots in silver nanowire bundles for surface-enhanced Raman spectroscopy. *J Am Chem Soc* 128:2200–2201
22. Imura K, Okamoto H, Hossain MK, Kitajima M (2006) Visualization of localized intense optical fields in single gold–nanoparticle assemblies and ultrasensitive Raman active sites. *Nano Lett* 6:2173–2176
23. Luo ZhH, Chen K, Lu DL, Han HY, Zou MQ (2011) Synthesis of p-aminothiophenol-embedded gold/silver core-shell nanostructures as novel SERS tags for biosensing applications. *Microchim Acta* 173:149–156
24. Yu XJ, Jiang ZhH, Wang QJ, Guo YSh (2010) Silver nanoparticle-based chemiluminescence enhancement for the determination of norfloxacin. *Microchim Acta* 171:17–22
25. Kim K, Park HK, Kim NH (2006) Silver-particle-based surface-enhanced Raman scattering spectroscopy for biomolecular sensing and recognition. *Langmuir* 22:3421–3427
26. Bogdanchikova NE, Kurbatov AV, Tret'yakov VV, Rodionov PP (1992) Activity of colloidal silver preparations towards smallpox virus. *Pharm Chem J* 26:778–779
27. Pietrobon B, McEachran M, Kitaev V (2009) Synthesis of size-controlled faceted pentagonal silver nanorods with tunable plasmonic properties and self-assembly of these nanorods. *ACS Nano* 3:21–26
28. Dieringer JA, McFarland AD, Shah NC, Stuart DA, Whitney AV, Yonzon CR, Young MA, Zhang X, Van Duyne RP (2006) Surface enhanced Raman spectroscopy: new materials, concepts, characterization tools, and applications. *Faraday Discuss* 132:9–26
29. Moskovits M (1985) Surface-enhanced spectroscopy. *Rev Mod Phys* 57:783–826
30. Otto A, Mrozek I, Grabhorn H, Akemann W (1992) Surface-enhanced Raman scattering. *J Phys Condens Matter* 4:1143–1212
31. Lee PC, Meise D (1982) Adsorption and surface-enhanced Raman of dyes on silver and gold sols. *J Phys Chem* 86:3391–3395
32. Kudelski A (2002) Raman and electrochemical characterization of 2-mercaptoethanesulfonate monolayers on silver: a comparison with monolayers of 3-mercaptopropionic acid. *Langmuir* 18:4741–4747
33. Kudelski A, Pecul M, Bukowska J (2002) Interaction of 2-mercaptoethanesulfonate monolayers on silver with sodium cations. *J Raman Spectrosc* 33:796–800
34. Li YS, Wang Y, Church JS, Garzena F, Zhang ZX, An DQ (2003) Vibrational spectroscopic studies of mesna and dimesna. *Spectrochim Acta Part A* 59:1791–1798
35. Wrzosek B, Bukowska J, Kudelski A (2005) Place-exchange reactions of thiols on electrochemically roughened SERS-active silver. *Vib Spectrosc* 39:257–261
36. Fujisawa K, Imai S, Suzuki S, Moro-oka Y, Miyashita Y, Yamada Y, Okamoto K (2000) M–S vibrational study in three-coordinate thiolato compounds (NEt₄)₂ [M(SC₆H₄-p-X)₃] and (NEt₄)₂ [M₄(m-SC₆H₄-p-Cl)₆]: M=Cu(I) and Ag(I), X=Cl and Br. *J Inorg Biochem* 82:229–238
37. Jeong DH, Jang NH, Suh JS (2000) Photodecomposition of diazanaphthalenes adsorbed on silver colloid surfaces. *J Phys Chem B* 104:3594–3600
38. Pergolese B, Muniz-Miranda M, Bigotto A (2005) Surface enhanced Raman scattering investigation of the halide anion effect on the adsorption of 1, 2,3-triazole on silver and gold colloidal nanoparticles. *J Phys Chem B* 109:9665–9671
39. Zamarion VM, Timm RA, Araki K, Toma HE (2008) Ultrasensitive SERS nanoprobe for hazardous metal ions based on trimercaptotriazine-modified gold nanoparticles. *Inorg Chem* 47:2934–2936
40. Wang L, Li T, Du Y, Chen CG, Li BL, Zhou M, Dong SJ (2010) Au NPs-enhanced surface plasmon resonance for sensitive detection of mercury(II) ions. *Biosens Bioelectron* 25:2622–2626
41. Liu ZD, Li YF, Ling J, Huang CZ (2009) A localized surface plasmon resonance light-scattering assay of mercury (II) on the basis of Hg²⁺-DNA complex induced aggregation of gold nanoparticles. *Environ Sci Technol* 43:5022–5027
42. Han DH, Kim Y-R, Oh J-W, Kim TH, Mahajan RK, Kim JS, Kim H (2009) A regenerative electrochemical sensor based on oligonucleotide for the selective determination of mercury (II). *Analyst* 134:1857–1862
43. Duan TC, Song XJ, Xu JW, Guo PR, Chen HT, Li HF (2006) Determination of Hg(II) in waters by on-line preconcentration using Cyanex 923 as a sorbent—cold vapor atomic absorption spectrometry. *Spectrochim Acta Part B* 61:1069–1073
44. Li J, Mei F, Li W-Y, He X-W, Zhang Y-K (2008) Study on the fluorescence resonance energy transfer between CdTe QDs and butyl-rhodamine B in the presence of CTMAB and its application on the detection of Hg(II). *Spectrochim Acta Part A* 70:811–817
45. Chen KH, Wang HW, Kang BS, Chang CY, Wang YL, Lele TP, Ren F, Pearton SJ, Dabiran A, Osinsky A, Chow PP (2008) Low Hg(II) ion concentration electrical detection with AlGaN/GaN high electron mobility transistors. *Sens Actuators B* 134:386–389
46. Yang FP, Ma Q, Yu W, Su XG (2011) Naked-eye colorimetric analysis of Hg²⁺ with bi-color CdTe quantum dots multilayer films. *Talanta* 84:411–415